applied sciences

MDPI

Article

A Tunable and Switchable Multi-Wavelength Erbium-Doped Fiber Ring Laser Enabled by Adjusting the Spectral Fringe Visibility of a Mach-Zehnder Fiber Interferometer

Romeo Emmanuel Nuñez Gomez [1], Gilberto Anzueto Sánchez [2], Alejando Martínez Ríos [2,*], Ariel Fong González [3], Alfredo Olarte Paredes [1], Areli Marlen Salgado Delgado [1], Jesús Castrellón Uribe [4] and René Salgado Delgado [1]

[1] Tecnológico Nacional de México/IT de Zacatepec, Calzada Tecnológico 27, Centro, Zacatepec de Hidalgo 62780, Morelos, Mexico; romeo.eng1@gmail.com (R.E.N.G.); alfredo.op@zacatepec.tecnm.mx (A.O.P.); areli.sd@zacatepec.tecnm.mx (A.M.S.D.); rene.sd@zacatepec.tecnm.mx (R.S.D.)
[2] Centro de Investigaciones en Óptica, A.C., León 37150, Guanajuato, Mexico; gilberto.anzueto@gmail.com
[3] Tecnológico Nacional de México/Instituto Tecnológico de Tuxtla Gutiérrez, Optomechatronic and Photonics Group, Postgraduate Department, Tuxtla Gutiérrez 29050, Chiapas, Mexico; fonga9692@gmail.com
[4] Centro de Investigación en Ingeniería y Ciencias Aplicadas (CIICAp), Universidad Autónoma del Estado de Morelos (UAEM), Cuernavaca 62209, Morelos, Mexico
* Correspondence: amr6@cio.mx

Abstract: This paper presents a tunable, switchable multi-wavelength emission from an erbium-doped fiber ring laser, enabled by adjusting the spectral fringe visibility of a fiber interferometer filter. The filter is formed with specially designed concatenated tapered fibers to configure a Mach-Zehnder fiber interferometer (MZFI). The laser emission is highly flexible and reconfigurable, allowing for tuning between single- and dual-wavelength operation. The laser can switch sequentially from one up to six wavelengths by fixing the curvature and adjusting the polarization state. The lasing emission is generated over a stable wavelength range between 1559.59 nm and 1563.54 nm, exhibiting an optical signal-to-noise ratio (OSNR) exceeding ~35 dB. The performance of amplitude and wavelength fluctuations were evaluated, indicating an appropriate stability of ~3 dB and a shift less than 0.1 nm within a 45 min period at room temperature. A detailed comparison with the literature is given.

Keywords: Mach-Zehnder fiber interferometer; tapered fibers; erbium-doped fiber laser; multi-wavelength; switchable laser

check for updates

Citation: Nuñez Gomez, R.E.; Anzueto Sánchez, G.; Martínez Ríos, A.; Fong González, A.; Olarte Paredes, A.; Salgado Delgado, A.M.; Castrellón Uribe, J.; Salgado Delgado, R. A Tunable and Switchable Multi-Wavelength Erbium-Doped Fiber Ring Laser Enabled by Adjusting the Spectral Fringe Visibility of a Mach-Zehnder Fiber Interferometer. *Appl. Sci.* **2024**, *14*, 9846. https://doi.org/10.3390/app14219846

Academic Editor: John Xiupu Zhang

Received: 19 September 2024
Revised: 23 October 2024
Accepted: 24 October 2024
Published: 28 October 2024

Copyright: © 2024 by the authors. Licensee MDPI, Basel, Switzerland. This article is an open access article distributed under the terms and conditions of the Creative Commons Attribution (CC BY) license (https://creativecommons.org/licenses/by/4.0/).

1. Introduction

Recently, considerable work has been done employing Mach-Zehnder fiber interferometers (MZFIs) based on two concatenated optical fiber tapers, which have been developed to enhance the lasing performance and functionalities in fiber laser systems. The filter operates by interfering with core and cladding modes. In the first taper, the core mode couples to higher-order cladding modes, acquiring a phase delay due to refractive index differences. The second taper reintroduces the cladding mode, forming a comb-like spectral pattern [1,2]. Typically, the MZFI is included as an intra-cavity filter in a fiber ring laser configuration. The tailorable filtering properties of MZFIs are explored in various forms. The first publication that employs an MZFI by concatenating two abrupt tapers separated by a section of SMF to demonstrate a tunable fiber laser was reported by X. Wang et al. in 2010 [3]. The tapers were fixed on positioning stages in that experiment, and adjustable bending was applied to the first taper. The amplified spontaneous emission of an erbium-doped fiber amplifier (EDFA) was reshaped into a comb-like transmission spectrum, and only higher-intensity peaks were amplified. As the taper's bending angle was increased, the lasing wavelength decreased consistently, tuning within the ~1550–1605 nm wavelength range. Pursuing this tendency, the same group reported the impact and optimization of the

waist diameter of tapered fibers and filter loss in an erbium-doped fiber ring laser (EDFRL), achieving a step-tunable performance from 1547.3 nm to 1563.4 nm [4].

Spectral features depend on taper dimensions and separation length. In this way, fiber spectral manipulation and laser wavelength performance rely, among other factors, on the variable that tunes the fiber filter, i.e., bending, strain, twist, or change in the external refractive index. For example, bending induces stress, thereby altering the effective refractive index of the interacting core and cladding modes and the geometrical dimensions influencing spectral transmission. Changes in the surrounding media also impact the filter's effective refractive index of the modes supported by the fiber structure. These factors have been utilized to demonstrate improved fiber lasers. For example, an EDFRL with a modified surrounding refractive index of the MZFI was reported in [5]. This modification involved gradually heating a glycerol solution to change the refractive index, achieving a wavelength tuning of 12 nm. A study in [6] also explored the immersion of an MZFI in combination with a fiber Bragg grating for a liquid-level fiber laser sensor, resulting in dual-wavelength modulation.

Conversely, switchable multi-wavelength lasers can be developed by leveraging the comb-like transmission spectrum. For instance, as described in Ref. [7], the realization of switchable multi-wavelength laser emission was successfully demonstrated by implementing a displacement S-bent MZFI configuration. This led to the simultaneous generation of four laser lines within an erbium ring cavity. Additionally, a tunable dual-laser emission spanning a range from 1520 nm to 1530 nm has been documented utilizing dual tapering of a 3 m section of Er-doped fiber [8] or a dual-wavelength single longitudinal mode from 1550 nm to 1554 nm EDFRL with Rayleigh backscattering assistance [9], and the use of mechanically bent in-line tapered MZFI to serve as a variable attenuator for dual wavelengths (1546.23 nm and 1554.76 nm) in an EDFRL [10].

Proposed experimental configurations also offer the capability for wavelength selectivity by tuning or generating multi-wavelength emissions ranging from ~1528 nm to 1562 nm. The proceeding was realized by superimposing two discrete free spectral ranges (FSR) and modifying the curvature of two MZFIs with dissimilar lengths between tapers connected in series [11]. In another approach, the application of external perturbations involving simultaneous changes in curvature and external refractive index directly affects the MZFI succeeding the adjustment of the FSR, extending the multi-wavelength emission in the C band (from ~1544.66 nm–1565.72 nm to ~1530.62nm–1565 nm) [12].

In works regarded with Ytterbium-doped fiber lasers, tunable dual-wavelength emission was performed with the aid of the MZFI and careful adjustments on the polarization states in the ring cavity [13], or applying tension or strain on the MZFI; spectral shifting was performed due to the adjustment of the birefringence within the Ytterbium ring cavity. This demonstrated a highly stable set of spacing tunable dual-wavelength emissions [14].

Alternatively, diverse setup configurations were designed to produce adjustable, tunable spacing dual-wavelength in EDFRLs, wherein the MZFI was driven by an acoustic transductor, as detailed in [15–17]. The versatility of integrating MZFI features with various wavelength-dependent fiber optic devices enhances the capability to control and manipulate laser wavelengths. Among the methods frequently utilized is the addition of a polarization controller (PC) to adjust the polarization state of light. This serves as an additional wavelength-dependent loss mechanism, enhancing the tunability and stability of the lasing wavelengths. In this aspect, experiments where the combination of the MZFI and the fine-tuning of the P.C. were implemented, and they reported the different configurations allow up to triple lasing wavelength with high wavelength stability and amplitude [18–22], and also for up to quadruple lasing wavelengths in thulium fiber lasers [23].

This work demonstrates a tunable and switchable multi-wavelength EDFRL progressing sequentially from single-wavelength to sextuple-wavelength emission. This is achieved using an MZFI as an intra-cavity filter which is formed by a pair of concatenated fiber tapers. Applying curvature to the MZFI increases spectral fringe visibility, allowing precise control over the tunable and multi-wavelength emissions through adjustments to both

the curvature and polarization state. The laser oscillation can be tuned from 1563.705 nm to 1558.05 nm, while four sets of switchable dual-wavelength emissions are attainable at 1543.21 nm and 1563.66 nm. Additionally, switchable emissions from single up to six wavelengths between 1559.59 and 1563.54 nm exhibit an optical signal-to-noise ratio of 38 dB. The system demonstrates stability, with amplitude variations of less than ~3 dB for most lasing wavelengths. This approach provides a versatile and cost-effective method to achieve tunable multi-wavelength laser oscillation by utilizing intra-cavity wavelength-dependent loss elements.

2. Experimental Setup

Figure 1 shows the experimental setup of the proposed tunable and switchable multi-wavelength EDFRL. Here, the gain medium is provided by 3 m of erbium-doped fiber with a large mode area (LIEKKI Er16-8/125), pumped with a pigtailed laser diode (L.D.) emitting at a central wavelength of 975 nm through a 980/1550 nm wavelength division multiplexer (WDM). A 3-paddle polarization controller (PC) is fusion spliced at the end of the erbium-doped fiber to adjust the polarization state. An optical coupler extracts 30% of the total light from the cavity and is processed with an optical spectrum analyzer (OSA Anritsu 9740A). The remaining 70% of the light is recirculated within the ring cavity. The MZFI is fusion spliced between the P.C. and the input port of the output coupler. Finally, an isolator is used to maintain unidirectional laser propagation.

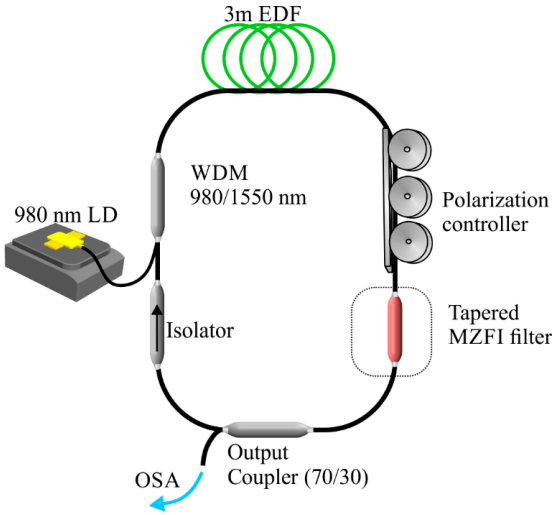

Figure 1. Experimental erbium-doped fiber ring laser cavity setup for tunable and multi-wavelength emission.

The MZFI operates based on the interference between the core and cladding modes, as shown in Figure 2a. In the first taper transition, the fundamental core mode transfers energy to high-order cladding modes, acquiring a phase difference while traveling through the region between tapers. Then, the energy is recoupled in the second taper transition and interacts with the core mode, creating an output spectra interference pattern. The proposed MZFI device comprises two equal quasi-abrupt concatenated tapered fiber sections fabricated from SMF-28 fiber using a GPX 3400 Vytran processing system. A crucial aspect of achieving optimal spectral characteristics and performance of the MZFI lies in the geometrical dimensions of each tapered section, described as follows: 2 mm transition length (T.L.), 1 mm waist length (W.L.), 60 µm waist diameter (W.D.), and 10 cm separation length (L) between tapers, as depicted in Figure 2a. The diameter is crucial for spectral positioning, the transition length affects the interference band size, and the waist length influences visibility, while the taper separation determines the fringe period as described in [24].

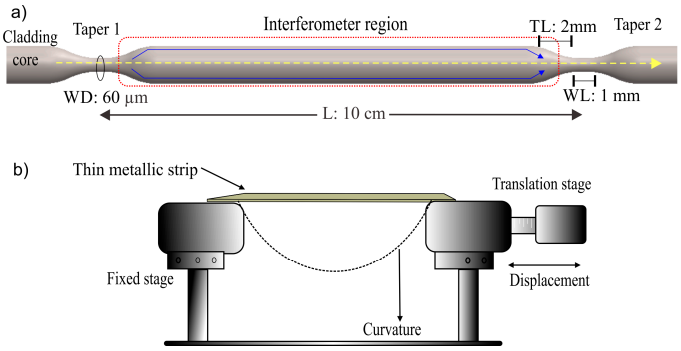

Figure 2. (**a**) MZFI structure formed with a pair of tapered sections fabricated on SMF-28, (**b**) displacement mechanism to used induce curvature in the MZFI.

Consequently, the MZFI was optimized to operate in the 1400–1600 nm range to interact with the Erbium ASE band. The filter undergoes controlled curvature to adjust the output spectral characteristics of the MZFI. The setup for applying curvature is depicted in Figure 2b, where the interferometer is positioned in a thin metallic strip and secured between two translation stages—one fixed, and the other capable of being displaced by a maximum of 2.54 cm—with a total separation of 30.5 cm.

3. MZFI Performance

The spectral response of the MZFI under controlled curvature conditions was measured using amplified spontaneous emission (ASE) from the erbium-doped fiber as the input light source before implementing the laser cavity. Figure 3 shows the baseline ASE spectrum (black line) and reshaped ASE (red line) obtained with the MZFI maintained straight (no curvature added). The reshaped ASE spectrum exhibits a weak comb-like shape from 1540 nm to 1560 nm. This phenomenon is due to the weak higher-order coupling modes resulting from the geometrical dimensions of the MZFI and the adiabaticity criteria (quasi-abrupt tapers) in the fabrication process [24]. The adiabaticity criteria define the gradual transition of fiber diameter in tapered structures, light mode propagation and coupling to higher-order modes. Quasi-abrupt tapers feature a slow tapering transition length that allows for weak higher-order coupling modes without significant energy loss.

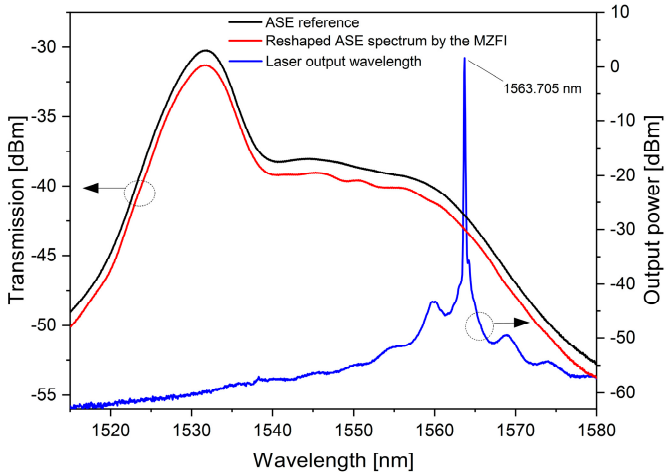

Figure 3. ASE spectrum as the light source from the EDF (black line) and the modified spectrum after passing through the MZFI (red line). The laser oscillation at 1563.07 nm is shown by the blue line.

Additionally, waist length, waist diameter, and separation taper length impact the comb-like spectrum's fringe visibility, spectral positioning, and free spectral range, necessitating a trade-off to achieve optimal light transmission and spectral characteristics. As the applied curvature increases, the stress induces a modification in the refractive index profile

via the elasto-optic effect, which reconfigures the spectral characteristics of the MZFI [25]. Consequently, according to [25], increased fringe visibility is expected to result in greater interference peaks and more defined comb shapes, highly desirable characteristics in multi-wavelength fiber lasers. The measured insertion loss of the MZFI was about ~1 dB. By closing the ring laser cavity and increasing the pump power to 40.5 mW, a single laser wavelength was stabilized at 1563.705 nm, reaching an OSNR of approximately 45 dB, as depicted by the blue line in Figure 3.

The controlled curvature was applied by displacing the translation stage in steps of approximately 1.27 mm. The curvature is inversely related to the bending radius and can be calculated using the expression [26]: $C = \frac{1}{R} = \sqrt{\frac{24x}{(L_0 - x)^3}}$, where L_0 represents the initial distance between the two mounts, x denotes the linear displacement of the translation stage, R is the bending radius, and C is the curvature in units of m^{-1}. Figure 4a depicts the modified ASE spectral transmission of the MZFI under different applied curvature levels (from 0 m^{-1} to 2.93 m^{-1}). As can be observed, a more defined comb-like spectral modulation is achieved by increasing the curvature, which strengthens the depth of the attenuation bands (increasing fringe visibility) and furthermore induces a wavelength shift. This detailed spectral response is shown in the inset of Figure 4b between the wavelengths of 1541 nm and 1560 nm. The same behavior occurs in all ASE spectra, but it is less apparent due to the peak shape between 1520 nm and 1540 nm and the marked intensity decrease beyond 1560 nm, resulting from the unique fluorescence emission of erbium-doped fiber (EDF). The measured free spectral range (FSR) is about 5 nm (inset Figure 4b) and remains relatively stable due to fiber curvature. In this context, the FSR mainly depends on the separation length between the tapers; a longer distance L results in a narrower FSR.

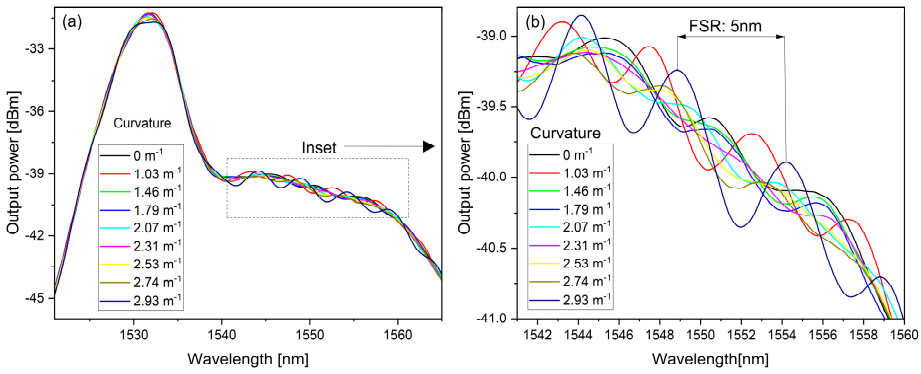

Figure 4. (**a**) The progressive modification of ASE spectrum with increasing curvature applied to the MZFI, (**b**) an inset in the range of 1541 to 1560 nm demonstrates an FSR of 5 nm.

It is crucial to characterize aspects such as the wavelength shift and fringe visibility in response to applied curvature. A blue shift is observed as the curvature is applied by selecting and monitoring the peak at 1555.8 nm (corresponding to 0 m^{-1}). The MZFI achieves a total wavelength shift of approximately 12 nm, as depicted by the black line in Figure 5. This behavior is highly advantageous for the generation of tunable and switchable multi-wavelength fiber emissions.

Fringe visibility, on the other hand, is a measure of the contrast between the interference quality patterns for interferometric systems. The visibility was determined using the established expression $V = \frac{I_{max} - I_{min}}{I_{max} + I_{min}}$, where I_{max} and I_{min} are the maximum and minimum intensities of the comb-like transmission output spectra [27]. The red line in Figure 5 shows that fringe visibility increases with curvature, reaching a maximum value of 0.56. This trend reflects the nonlinear relationship between curvature and fringe visibility. Specifically, the visibility rises as curvature increases, indicating an enhanced mode coupling efficiency. However, this effect is not linear, as fringe visibility can both increase and decrease with varying curvature values. This behavior stems from the complex interplay

between curvature-induced stress and its impact on the effective refractive index, which affects the mode coupling efficiency.

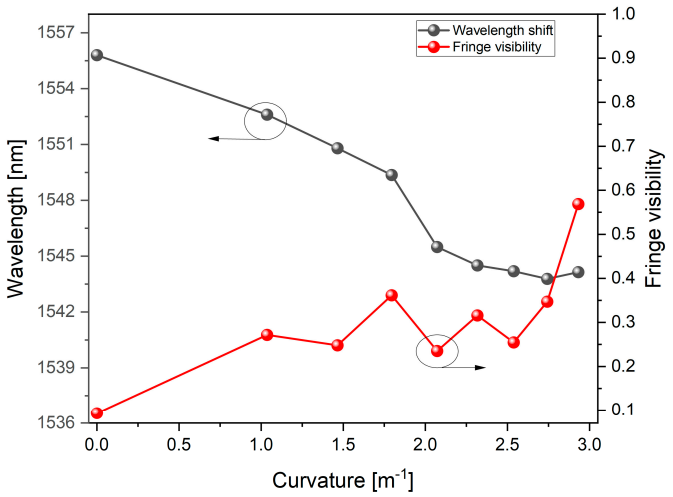

Figure 5. The wavelength shifts as a function of curvature (0 m^{-1} to 2.93 m^{-1}) and the variation of the measured fringe visibility.

Fringe visibility plays a crucial role in the performance of fiber lasers. An increase in fringe visibility leads to a more defined interference pattern, enhancing the laser cavity's feedback mechanism. This improvement directly influences key parameters like the OSNR and the side mode suppression ratio (SMSR), as a stronger interference pattern helps amplify the desired signal wavelengths while suppressing noise and unwanted side modes. Consequently, this enhanced control over the laser's feedback facilitates the generation of multi-wavelength, switchable, or tunable lasers with greater stability and precision.

4. Tunable and Switchable Performance

Following the evaluation of the filter performance, the ring cavity was closed and the pump power was adjusted to 50.6 mW; single-wavelength laser oscillation at 1563.705 nm was achieved (refer to Figure 3).

The fiber laser performance was evaluated by increasing the curvature level of the MZFI from 0 m^{-1} to 2.79 m^{-1}. During the process, distinct output laser characteristics were observed, including tunable single-wavelength, dual-switchable, and switchable multi-wavelength emissions with up to six wavelengths. Figure 6 displays the tunable single emission ranging from 1563.705 nm to 1558.05 nm when the curvature is gradually increased from 0 m^{-1} to 1.97 m^{-1}, resulting in a maximum tunable range of 5.65 nm. The measured OSNR is about 55 dB for most of the lasing wavelengths, while the amplitude power difference of each wavelength is less than 1.6 dB.

In contrast, four sets of switchable dual-wavelength emissions were generated between 1543.21 nm and 1563.66 nm for curvatures of 1.53 m^{-1}, 2.33 m^{-1}, 2.5 m^{-1}, and 2.75 m^{-1}, as depicted in Figure 7. The wavelength separations were as follows: 4.59 nm for 1.53 m^{-1} (1559.07 nm and 1563.66 nm, Figure 7a), 6.07 nm for 2.33 m^{-1} (1543.21 nm and 1549.287 nm, Figure 7b), 5.05 nm for 2.5 m^{-1} (1554.61 nm and 1559.667 nm, Figure 7c), and 5.01 nm for 2.75 m^{-1} (1556.8 nm and 1561.877 nm, Figure 7d). These lasing wavelengths demonstrated an optical signal-to-noise ratio (OSNR) above 40 dB.

The curvature was carefully increased to 2.363 m^{-1} to induce switchable multi-wavelength laser emission. This adjustment caused the lasing line to exhibit a slight blue shift, resulting in a single wavelength centered at 1562.22 nm with an amplitude of 38.4 dB, as illustrated in Figure 8a. From the figure, the optical spectrum in the range of 1558 nm to 1567 nm exhibits a slight comb-like pattern with a flattened profile at the upper portion. This effect, resulting from the MZFI being subjected to curvature, leads to a flattened gain profile of the erbium-doped fiber, thereby promoting mode competition

and allowing multiple longitudinal modes to oscillate simultaneously. These adjacent modes, observable in both directions relative to the actual laser emission, can be further amplified to generate more laser lines by precisely controlling the polarization states and the curvature applied to the MZFI.

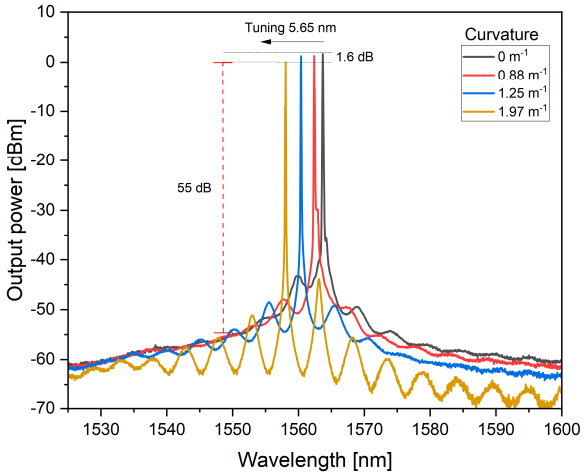

Figure 6. Tunable single laser wavelength between 1563.705 nm to 1558.05 nm for the curvatures from 0 m^{-1} to 2.79 m^{-1}.

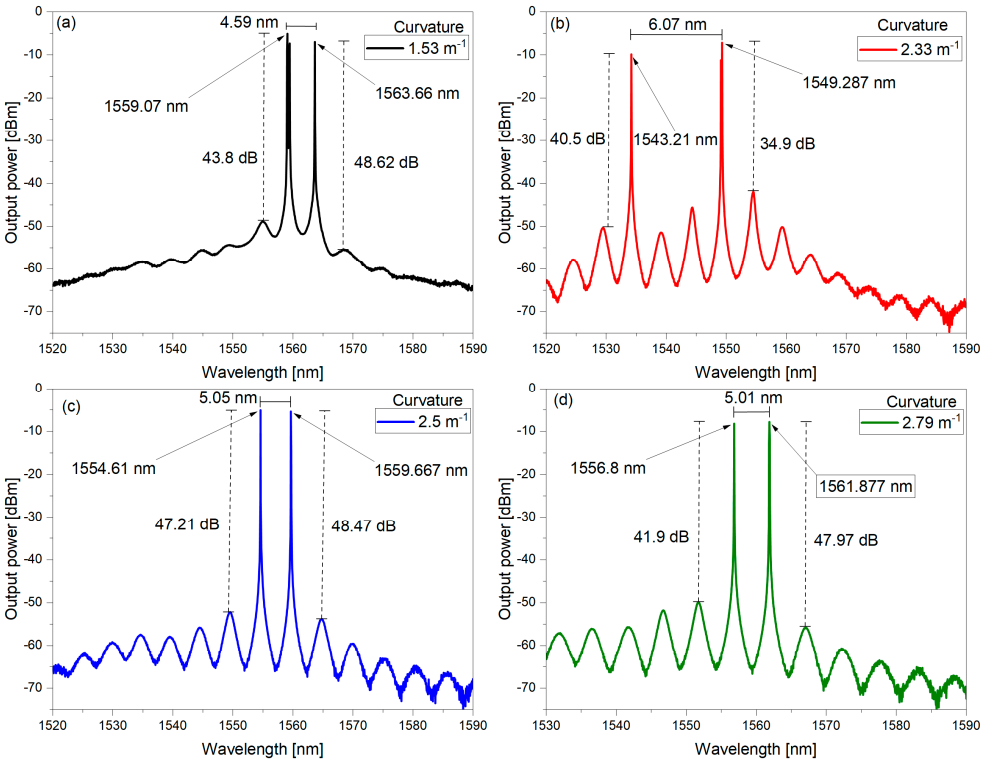

Figure 7. (**a**). Switchable dual-wavelength emissions generated at curvatures of 1.53 m^{-1} with 1559.07 nm and 1563.66 nm, (**b**) 2.33 m^{-1} with 1543.21 nm and 1549.287 nm, (**c**) 2.5 m^{-1} with 1554.61 nm and 1559.667 nm, (**d**) 2.75 m^{-1} with 1556.8 nm and 1561.877 nm.

By maintaining the current curvature and adjusting the polarization state via P.C., switchable multi-wavelength laser emission was realized, resulting in the sequential production of laser lines. Dual-wavelength (1562.22–1562.875 nm), triple-wavelength (1560.175–1562.22–1562.88 nm) and quadruple-wavelength (1560.85–1561.51–1562.26–1562.86 nm)

emissions were obtained, as shown in Figure 8b,c and Figure 9a, with an OSNR of 35.7 dB, 35 dB, 34.9 dB, respectively.

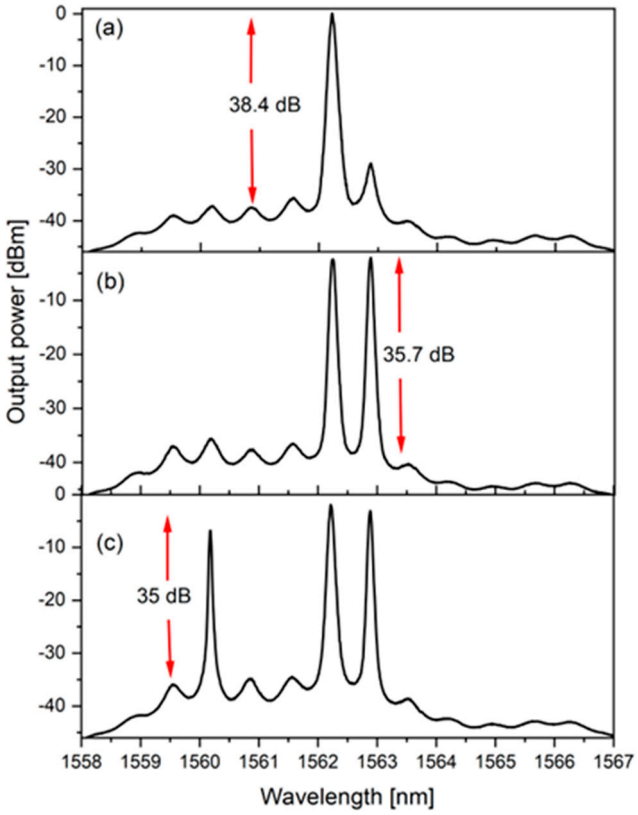

Figure 8. (**a**) Single-wavelength oscillation at 1562.22 nm, (**b**) dual-wavelength oscillation (1562.22–1562.875 nm), (**c**) triple-wavelength oscillation (1560.175–1562.22–1562.88 nm).

To excite and amplify additional adjacent modes beyond the quadruple-wavelength laser emission, the curvature was slightly adjusted to 2.417 m^{-1}. This adjustment resulted in a slight gain flattening across the spectral range of the multi-wavelength emission.

As depicted in Figure 9b,c, when combined with a gradual adjustment of the polarization state, this change facilitated the generation of five-wavelength (1559.59–1560.91–1561.58–1562.93–1563.61 nm) and six-wavelength (1560.25–1560.97–1561.63–1562.29–1562.98–1563.64 nm) laser oscillations with OSNR of 35 dB.

The FSR between adjacent laser lines was measured to be approximately 0.66 nm. The maximum spectral distance achieved between laser lines was about 4.05 nm.

Ensuring the stability of multi-wavelength laser emission is crucial for consistent performance across various applications. Stability characterization is essential for evaluating how the laser is affected by environmental conditions, which is critical to maintaining the integrity of the laser system and ensuring that outputs are consistently reliable and repeatable. For a detailed assessment of amplitude and wavelength stability, nine sequential scans of the lasing spectra were conducted at 5 min intervals, comprehensively covering all the obtained multi-wavelength spectra.

Figure 10 illustrates the spectral distribution stability of a single laser oscillation at 1562.22 nm, showing high-intensity uniformity across the spectrum. Figure 10b shows a maximum wavelength shift of 0.01 nm, while Figure 10c presents output power fluctuations of less than 0.12 dB, reflecting consistent power.

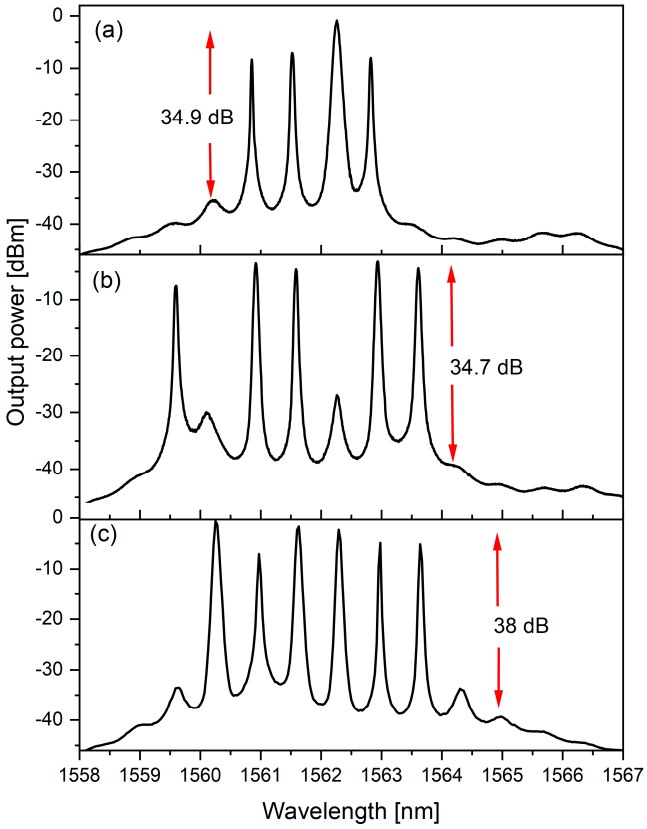

Figure 9. (**a**) Quadruple-wavelength emission (1560.85–1561.51–1562.26–1562.86 nm), (**b**) quintuple-wavelength emission (1559.59–1560.91–1561.58–1562.93–1563.61 nm), and (**c**) sextuple-wavelength emission (1560.25–1560.97–1561.63–1562.29–1562.98–1563.64 nm).

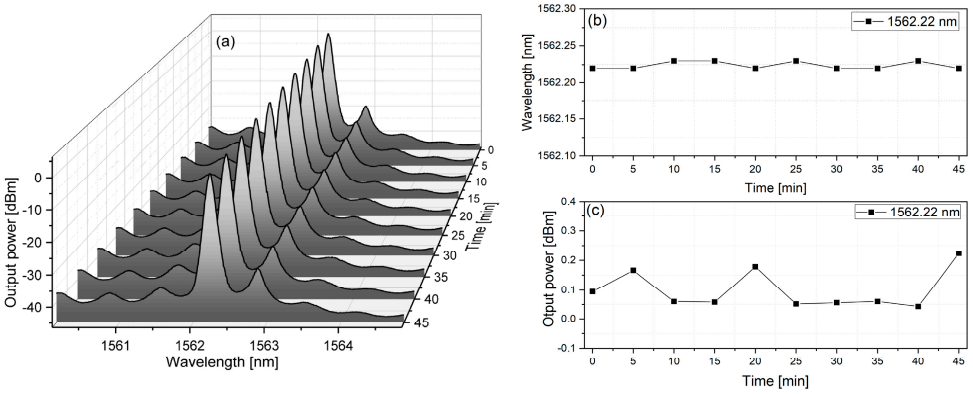

Figure 10. (**a**) Spectral distribution stability of a single laser oscillation at 1562.22 nm, with high-intensity uniformity across the spectrum, (**b**) a maximum wavelength shift of 0.01 nm, and (**c**) output power fluctuations of less than 0.12 dB.

Figure 11a presents the power spectrum of the dual-wavelength laser. The lasing lines centered at approximately 1562.22 nm and 1562.875 nm exhibit a wavelength shift of approximately 0.07 nm, as observed in Figure 11b. Figure 11c illustrates the power fluctuations of the two lasing lines, with maximum values of 1.11 dB and 0.25 dB, respectively.

Figure 12 presents the power stability characteristics exhibited by the triple-wavelength laser system. An evaluation of the 1560.182 nm laser line reveals a maximum wavelength shift of 0.07 nm (Figure 12b) and a maximum amplitude fluctuation of 0.51 dB (Figure 12c). It is important to note that the remaining wavelengths in the triple-wavelength configura-

tion demonstrated power stability levels exceeding the measurement parameters, indicating superior performance for those specific lines.

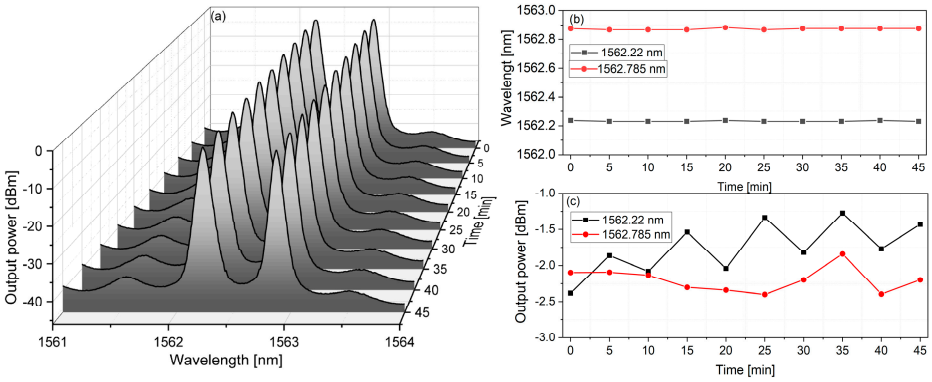

Figure 11. (**a**). Stability of the dual-wavelength laser oscillation at 1562.22–1562.785 nm with uniform intensity, (**b**) a maximum wavelength shift of 0.07 nm, and (**c**) output power fluctuations of less than 0.25 dB.

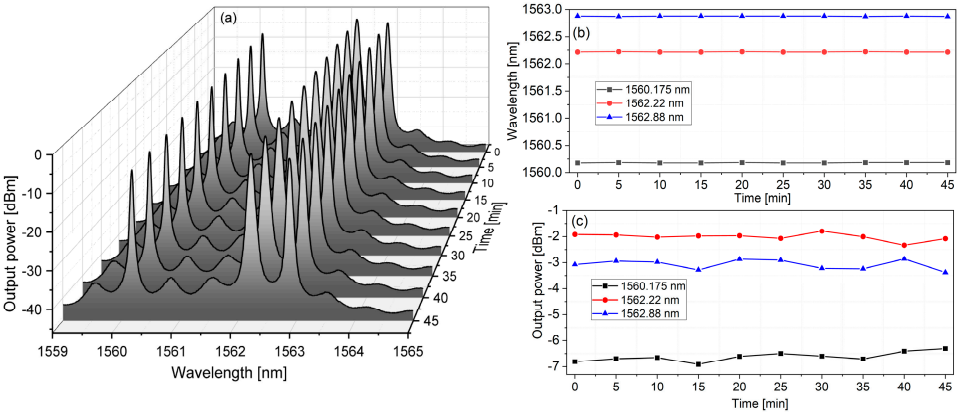

Figure 12. (**a**) Power stability of the triple-wavelength laser system, (**b**) maximum wavelength shift of 0.07 nm, and (**c**) maximum amplitude fluctuation of 0.51dB for the 1562.88 nm line.

Additionally, the stability of the four-wavelength emission is presented in Figure 13. In this case, the maximum wavelength shift is approximately 0.022 nm for the wavelength at 1562.83 nm, indicated by the blue line with triangular markers in Figure 13b. This wavelength also exhibits the most considerable fluctuation in power, with a maximum variation of 3 dB, as shown in Figure 13c.

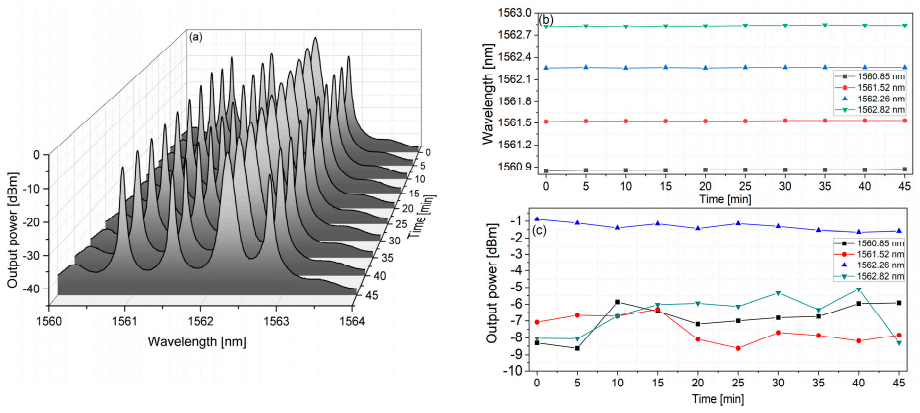

Figure 13. (**a**) Power stability of the quadruple-wavelength laser system, (**b**) maximum wavelength shift of 0.22 nm, and (**c**) maximum amplitude fluctuation of 3 dB for the 1562.83 nm line.

For the following quintuple-wavelength and sextuple-wavelength stability analyses, as shown in Figures 14 and 15, the maximum wavelength shift of 0.07 nm was estimated at 1562.93 nm (indicated by the pink dotted line in Figure 14b). The maximum amplitude deviation recorded was 1.7 dB for the wavelength of 1561.58 nm, as depicted in Figure 14c. For the sextuple-wavelength configuration, the wavelength shift was effectively negligible, while a maximum power fluctuation of 2.71 dB was noted at the wavelength of 1562.98 nm, as illustrated in Figures 15b and 15c, respectively.

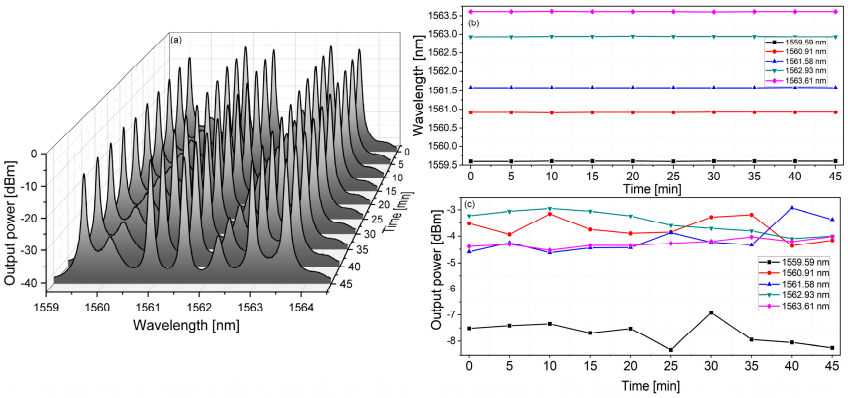

Figure 14. (**a**) Power stability of the quintuple-wavelength laser system, (**b**) maximum wavelength shift of 0.07 nm, and (**c**) maximum amplitude fluctuation of 1.7 dB for the 1561.58 nm line.

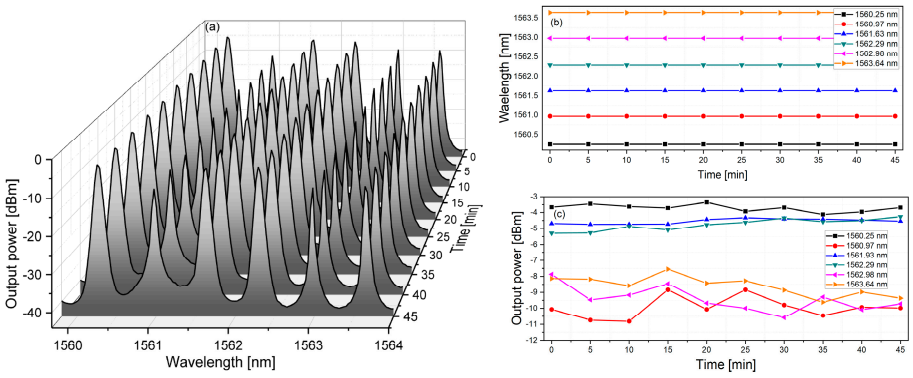

Figure 15. (**a**) Power stability of the sextuple-wavelength laser system, (**b**) negligible wavelength shift, and (**c**) maximum amplitude fluctuation of 2.71 dB for the 1562.98 nm line.

Overall, these results highlight a notable stability as the number of lasing wavelengths increases, demonstrating the effectiveness of this approach in improving the performance and reliability of the switchable multi-wavelength laser system. The observed stability underscores the system's robustness, reflecting its ability to maintain consistent operation across a broad lasing spectral range.

5. Discussion

The observed ability to tune the laser, produce switchable dual wavelengths, and sequentially switch between multiple wavelengths is due to the combined effects of the MZFI's spectral shaping, the EDF gain dynamics, and intracavity polarization control. The MZFI generates a comb-like spectrum through periodic phase shifts and interference resulting from the designed geometry and changes in the effective refractive index of the coupled light modes due to the elasto-optic effect produced by inducing curvature. As curvature increases, these modifications make a series of spectral peaks corresponding to resonance conditions for specific wavelengths. Figures 4 and 5 illustrate that increased curvature enhances the prominence of the comb-like spectrum, improves fringe visibility, and causes observable wavelength shifts, indicating the system's sensitivity to curvature

changes. Minor variations in visibility or wavelength shifts can redistribute the EDF gain profile, preferentially enhancing laser oscillation and stabilization at the comb peaks. At relatively low curvatures (Figure 6), while fringe visibility is still insufficient for multi-wavelength oscillation, spectral shifts still occur, resulting in a single wavelength tuning by 5.65 nm with an optical OSNR above 50 dB. At higher curvature levels, there is a notable increase in fringe visibility, with the switchable dual-wavelength emission feature becoming evident in the 1543.21 nm and 1563.66 nm range (Figure 7) with an OSNR exceeding 40 dB. The increased curvature refines the spectral comb pattern and adjusts the gain profile, supporting the dual-wavelength operation and improving laser performance.

The switchable multi-wavelength performance is caused when the curvature is adjusted at 2.363 m^{-1}, producing a comb-like output showing a flattened profile. This effect is clearly comparable with the profile at 2.31 m^{-1} from Figure 4b (pink line), where the comb-like spectrum is reduced (visibility of 0.35), leading to consistent gain across the spectral lasing peak (see Figure 8a). The reduction in visibility likely indicates a more uniform distribution of the optical power across the spectrum. This condition promotes strong mode competition within the laser cavity, causing side modes to oscillate as the gain flattening equalizes the lasing conditions for multiple wavelengths. Simultaneously, by fine-tuning the polarization state, the side modes experience more favorable conditions for amplification by receiving sufficient gain to exceed the lasing threshold, resulting in the excitation of additional lasing wavelengths to be selected sequentially. The demonstrated stability of this configuration highlights its suitability for advanced multi-wavelength laser systems, meeting rigorous performance benchmarks.

Stability is essential for reliable operation, validating system performance, and ensuring consistent output in practical applications. Several external factors can significantly influence stability variations. Small mechanical vibrations arising from the manipulation of setup components can disrupt stability. Temperature fluctuations in the surrounding medium of the tapered region can induce thermal expansion, altering the path length of the MZFI, and the effect of humidity can affect their refractive index and transmission properties. Furthermore, fluctuations in pump power can contribute to these instabilities, affecting the system's overall performance. The approach's robustness and adaptability confirm its effectiveness, making it a superior choice for high-performance laser systems and paving the way for future advancements.

Our proposal leverages the simplicity, relatively low cost, and versatility of a single intra-cavity filter with comb-like spectral features for tunable and multi-wavelength emission. This approach offers significant advantages over complex, hard-to-manufacture systems. For example, a two-mode fiber section spliced between SMF segments requires long nonlinear fiber (120 m) or SMF (3 km) to generate up to 10 lasing wavelengths with relatively high power fluctuations [28]. Other methods, like triple-core photonic crystal fiber or cascaded LPFGs, achieve fewer switchable wavelengths [29] and limited tunability due to the spectral finesse [30]. Twin photonic crystal fiber filters can achieve SMSRs above 57 dB for single-wavelength and 40 dB for multi-wavelength emission, though stability fluctuations reach 8.09 dB [31]. The SMF-SCF-SMF structure with enlarged splices allows tunable and multi-wavelength features via temperature, curvature, and polarization perturbations [32]. However, cross-sensitivities may affect output performance. Asymmetric LPFG demonstrates switchable multi-wavelength performance up to six wavelengths sequentially, comparable to the performance achieved in our research, but with larger output power variations of up to 6 dB [33]. The MMF-PMF-MMF filter induces the PHB effect for tunable single to sextuple wavelengths, requiring modification of the cavity by adding a Sagnac filter, complicating the design [34]. Our results demonstrate comparable or superior performance to previous studies, achieving superior stability with less complicated and relatively low-cost filters. Enhanced wavelength performance, characterized by precise tuning and minimal drift, makes this design an efficient and reliable solution for various practical applications. Compared to more complex designs, our approach offers significant advantages in terms of stability, performance, and cost-effectiveness.

Finally, a comparative analysis of the tunable, switchable multi-wavelength fiber laser versus those utilizing concatenated tapered fibers and other structures is presented and summarized in Table 1. The study covers key aspects such as fiber filter structures, operational wavelengths, performance metrics, side-mode suppression ratios, and stability, highlighting significant differences and advantages. This examination emphasizes the impact of these factors on optimizing laser functionality and performance.

Table 1. Comparative analysis of tunable, switchable multi-wavelength fiber lasers with concatenated tapered fibers and other structures, highlighting key parameters such as filter configurations, wavelengths, performance, side-mode suppression, and stability.

Ref	Filter Type	Laser Performance	Laser Lines	Wavelength Operation	SMSR	Power Fluctuation	Wavelength Fluctuations	Control
This work	MZFI pair of concatenated tapered fibers	Tunable single/switchable M.W.	6	1543.21–1563.705nm	40 dB	3 dB	0.07 nm	Curvature Polarization
[17]	AO-MZI taper-shaped sandwich-like fiber	Tunable/switchable dual W	2	1563.82–1569.16 nm	40 dB	3 dB	0.02 nm	Acousto-optic
[20]	Two-taper MZFI	Switchable M.W.	3	1557.2–1570.2 nm	33.72 dB	2.482 dB	—	Polarization
[21]	Dual biconical fiber taper	Switchable M.W.	3	1978.8–1991.8 nm	30 dB	4.73 dB	Negligible	Polarization
[22]	IFMZI based on ABTF	Switchable M.W.	3	1558.36–1562.36 nm	51.1 dB	1.64 dB	0.76 nm	Polarization
[23]	Two-taper fiber	Tunable single/switchable M.W.	6	1952.06–1975.62 nm	31.87 dB	0.9 dB	0.3 nm	Polarization
[28]	TMF core offset structure	Switchable M.W.	10	1550.56–1553.77 nm	30 dB	3.82 dB	0.01 nm	Polarization
[29]	TCPCF and MMF segment	Tunable single/switchable M.W.	3	1540.32–1568.9 nm	50 dB	0.96 dB	0.06 nm	Strain Polarization
[30]	Cascaded FBG	Switchable M.W.	4	1550–1562 nm	47 dB	0.966 dB	0.044 nm	Polarization
[31]	TCPCF and SLF	Tunable single/tunable switchable W.M.	3	1531–1568.5 nm	40 dB	8.09 dB	0.09 nm	Bending Polarization
[32]	MZI based on SCF and waist enlarged	Tunable single/switchable M.W.	3	1539.36–159.63 nm	51 dB	1.344 dB	0.1479 nm	Temperature Curvature Polarization
[33]	Asymmetrically LPFG	Switchable M.W.	6	1546–1553 nm	38.02 dB	6.9 dB	0.28 nm	Curvature
[34]	MMF–PMF–MMF	Switchable M.W.	6	1528.73–1560.99 nm	41 dB	0.1 dB	0.15 nm	Polarization
[35]	MZFI two waist enlarged bi-taper	Tunable singe/switchable M.W.	3	1554.4–1563.5 nm	30 dB	0.59 dB	—	Polarization
[36]	MZI based on two-taper	Tunable/switchable W.M.	4	1527–1563 nm	15 dB	2.98 dB	0.71 nm	Curvature
[37]	MZI and S.I. bi-tapered PMFs	Switchable M.W.	3	1530.1–1560.8 nm	42.2 dB	Not reported	Not reported	Polarization
[38]	MZFI bi-tapered PFMs	Q-switched/switchable M.W.	4	1529.8–1532.9 nm	34.9 dB	—	—	Polarization
[39]	FPI and MZFI	Switchable M.W.	4	1525-1534 nm	30 dB	1.2 dB	0.05 nm	Curvature
[40]	Sagngac and Lyot filters	Tunable/switchable M.W.	7	1530–1560 nm	40 dB	3 dB	0.4 nm	Polarization

Table 1. *Cont.*

Ref	Filter Type	Laser Performance	Laser Lines	Wavelength Operation	SMSR	Power Fluctuation	Wavelength Fluctuations	Control
[41]	Core offset MZI based on NZ-DSF	Switchable M.W.	3	1546–1564 nm	56 dB	2.2 dB	0.02 nm	Polarization
[42]	Core offset ACMZFI	Tunable single/switchable M.W.	3	1557–1562.32 nm	55 dB	5 dB	0.02 nm	Temperature Polarization
[43]	SE-HSOFF	Switchable/tunable M.W.	4	1526.2–1556.3 nm	30 dB	1.93 dB	0.1 nm	Polarization
[44]	PSBG and MZI	Tunable/switchable M.W.	4	1527–1550 nm	50 dB	Not reported	0.025 nm	Optical attenuation Temperature Strain

6. Conclusions

In conclusion, this study successfully implements a tunable and switchable multi-wavelength erbium-doped fiber ring laser (EDFRL) based on an MZFI formed with a pair of tapered fibers. The system allows wavelength-switching from a single wavelength to up to six wavelengths by adjusting the fringe visibility of the MZFI and the polarization state, covering a spectral range from 1543.21 nm to 1563.705 nm. Our results show that the laser exhibits excellent power stability, with fluctuations typically less than 3 dB and some wavelengths showing variations of less than 0.7 dB at room temperature. The simplicity and low cost of the fabrication process offer significant advantages over more complex systems. Additionally, the performance and stability of our design are competitive and, in many aspects, align with those reported in the literature.

Author Contributions: Conceptualization, G.A.S. and A.M.R.; Methodology, R.E.N.G., A.M.R. and A.F.G.; Validation, G.A.S.; Formal analysis, G.A.S. and A.M.R.; Investigation, R.E.N.G., G.A.S., A.M.R., A.O.P., A.M.S.D., J.C.U. and R.S.D.; Data curation, G.A.S.; Writing—original draft, R.E.N.G., G.A.S. and A.M.R.; Writing—review & editing, R.E.N.G., G.A.S. and A.M.R.; Project administration, G.A.S.; Funding acquisition, G.A.S. All authors have read and agreed to the published version of the manuscript.

Funding: This research was funded by the Consejo Nacional de Humanidades, Ciencias y Tecnologías (CONAHCYT) in Mexico.

Institutional Review Board Statement: Not applicable.

Informed Consent Statement: Not applicable.

Data Availability Statement: The raw data supporting the conclusions of this article will be made available by the authors upon request.

Conflicts of Interest: The authors declare no conflict of interest.

References

1. Bhardwaj, V.; Kishor, K.; Sharma, A.C. Tapered optical fiber geometries and sensing applications based on Mach Zehnder Interferometer: A review. *Opt. Fiber Technol.* **2020**, *58*, 102302. [CrossRef]
2. Wang, Q.; Wei, W.; Guo, M.; Zhao, Y. Optimization of cascaded fiber tapered Mach-Zehnder interferometer and refractive index sensing technology. *Sens. Actuators B Chem.* **2016**, *222*, 159–165. [CrossRef]
3. Wang, X.; Li, Y.; Bao, X. C- and L-band tunable fiber ring laser using a two-taper Mach–Zehnder interferometer filter. *Opt. Lett.* **2010**, *35*, 3354. [CrossRef] [PubMed]
4. Yin, G.; Wang, X.; Bao, X. Effect of beam waists on performance of the tunable fiber laser based on in-line two-taper Mach-Zehnder interferometer filter. *Appl. Opt.* **2011**, *50*, 5714–5720. [CrossRef]
5. Selvas-Aguilar, R.; Martínez-Rios, A.; Anzueto-Sánchez, G.; Castillo-Guzmán, A.; Hernández-Luna, M.C.; Robledo-Fava, R. Tuning of an erbium-doped fiber ring laser based on heating a tapered fiber filter. *Opt. Fiber Technol.* **2014**, *20*, 391–394. [CrossRef]
6. Zhang, W.; Ying, Z.; Yuan, S.; Tong, Z. A fiber laser sensor for liquid level and temperature based on two taper structures and fiber Bragg grating. *Opt. Commun.* **2015**, *342*, 243–246. [CrossRef]

7. Martinez-Rios, A.; Anzueto-Sanchez, G.; Monzon-Hernandez, D.; Salceda-Delgado, G.; Castrellon-Uribe, J. Multi-wavelength switching of an EDFL by using a fixed fiber-comb filter and a broadband tunable S-bent fiber filter. *Opt. Laser Technol.* **2014**, *58*, 197–201. [CrossRef]
8. Ali, M.I.M.; Ibrahim, S.A.; Abu Bakar, M.H.; Noor, A.S.M.; Anas, S.B.A.; Zamzuri, A.K.; Mahdi, M.A. Tapered-EDF-Based Mach-Zehnder Interferometer for Dual-Wavelength Fiber Laser. *IEEE Photonics J.* **2014**, *6*, 1–9. [CrossRef]
9. Gu, J.; Yang, Y.; Liu, M.; Zhang, J.; Wang, X.; Yuan, Y.; Yao, Y. A switchable and stable single-longitudinal-mode, dual-wavelength erbium-doped fiber laser assisted by Rayleigh backscattering in tapered fiber. *J. Appl. Phys.* **2015**, *118*, 103107. [CrossRef]
10. Tan, S.; Yan, F.; Li, Q.; Peng, W.; Liu, S.; Feng, T.; Chang, F. A stable single-longitudinal-mode dual-wavelength erbium-doped fiber ring laser with superimposed FBG and an in-line two-taper MZI filter. *Laser Phys.* **2013**, *23*, 3–8. [CrossRef]
11. Nunez-Gomez, R.E.; Anzueto-Sanchez, G.; Martinez-Rios, A.; Basurto-Pensado, M.A.; Castrellon-Uribe, J.; Camas-Anzueto, J. Combining comb-filters based on tapered fibers for selective lasing performance in erbium-doped fiber lasers. *Laser Phys.* **2016**, *26*, 125101. [CrossRef]
12. Nuñez-Gomez, R.E.; Anzueto-Sanchez, G.; Martinez-Rios, A.; Basurto-Pensado, M.A.; Castrellon-Uribe, J.; Selvas-Aguilar, R.; Camas-Anzueto, J.; Duran-Ramirez, V.M. Multi-wavelength switching of an erbium-doped fiber ring laser based on the cross-sensitivities' features of tapered fiber filters. *Opt. Rev.* **2015**, *22*, 526–531. [CrossRef]
13. Ahmad, H.; Salim, M.A.; Azzuhri, S.R.; Zulkifli, M.Z.; Harun, S.W. Dual wavelength single longitudinal mode ytterbium-doped fiber laser using a dual-tapered Mach-Zehnder interferometer. *J. Eur. Opt. Soc.* **2015**, *10*, 15013. [CrossRef]
14. Ahmad, H.; Salim, M.A.M.; Azzuhri, S.R.; Jaddoa, M.F.; Harun, S.W. Tunable dual-wavelength ytterbium-doped fiber laser using a strain technique on microfiber Mach–Zehnder interferometer. *Appl. Opt.* **2016**, *55*, 778. [CrossRef] [PubMed]
15. Yan, N.; Han, X.; Chang, P.; Huang, L.; Gao, F.; Yu, X.; Zhang, W.; Zhang, Z.; Zhang, G.; Xu, J. Tunable dual-wavelength fiber laser with unique gain system based on in-fiber acousto-optic Mach–Zehnder interferometer. *Opt. Express* **2017**, *25*, 27609. [CrossRef]
16. Huang, L.; Chang, P.; Song, X.; Peng, W.; Zhang, W.; Gao, F.; Bo, F.; Zhang, G.; Xu, J. Tunable in-fiber Mach-Zehnder interferometer driven by unique acoustic transducer and its application in tunable multi-wavelength laser. *Opt. Express* **2016**, *24*, 2406. [CrossRef]
17. Han, X.; Wang, Z.; Gao, F.; Zhang, W.; Bo, F.; Dong, X.; Zhang, G.; Xu, J. Robust and low cost in-fiber acousto-optic Mach–Zehnder interferometer and its application in a dual-wavelength laser. *Appl. Opt.* **2021**, *61*, 22. [CrossRef]
18. He, W.; Yuan, H.; Lou, X.; Zhu, L.; Dong, M. Multi-wavelength switchable erbium-doped fiber laser based on a hybrid filter incorporating a bi-tapered Mach-Zehnder interferometer and Sagnac loop. *Phys. Scr.* **2019**, *94*, 125502. [CrossRef]
19. Peng, W.; Liu, P. Multi-wavelength erbium-doped fiber laser based on a polarization-dependent in-line Mach–Zehnder interferometer. *Opt. Quantum Electron.* **2019**, *51*, 300. [CrossRef]
20. Wei, H.; Lianqing, Z.; Mingli, D. All-fiber Mach–Zehnder comb filter based on tapered fibers for wavelength switchable erbium-doped fiber lasers. *Int. J. Optomechatron.* **2020**, *14*, 18–28. [CrossRef]
21. Wu, X.; Miao, J.; Wang, Y.; Chen, W.; Chen, Z. All-fiber theta cavity multi-wavelength Tm-doped fiber laser based on a dual biconical taper filter. *Opt. Fiber Technol.* **2020**, *60*, 102331. [CrossRef]
22. Geng, X.; Jiang, Y.; Gu, H.; Luo, S.; Sun, M.; Li, L. Switchable multi-wavelength fiber lasers based on asymmetric biconical fiber tapers. *Opt. Commun.* **2023**, *548*, 129837. [CrossRef]
23. Li, T.; Yan, F.; Wang, P.; Wang, X.; Suo, Y.; Zhou, H. Switchable Multi-Wavelength Thulium-Doped Fiber Laser using a Two-Taper fiber filter. *Infrared Phys. Technol.* **2022**, *125*, 104269. [CrossRef]
24. Salceda-Delgado, G.; Martinez-Rios, A.; Monzón-Hernández, D. Tailoring Mach-Zehnder comb-filters based on concatenated tapers. *J. Light. Technol.* **2013**, *31*, 761–767. [CrossRef]
25. Monzon-Hernandez, D.; Martinez-Rios, A.; Torres-Gomez, I.; Salceda-Delgado, G. Compact optical fiber curvature sensor based on concatenating two tapers. *Opt. Lett.* **2011**, *36*, 4380. [CrossRef]
26. Wang, Q.; Liu, Y. Review of optical fiber bending/curvature sensor. *Measurement* **2018**, *130*, 161–176. [CrossRef]
27. Hecht, E. *Optics*, 5th ed. Pearson Education, Adelphi University. 2017. Available online: https://www.pearson.com/en-us/subject-catalog/p/optics/P200000006793/9780137526420 (accessed on 15 October 2024).
28. Zhao, Q.; Pei, L.; Tang, M.; Xie, Y.; Ruan, Z.; Zheng, J.; Ning, T. Switchable multi-wavelength erbium-doped fiber laser based on core-offset structure and four-wave-mixing effect. *Opt. Fiber Technol.* **2020**, *54*, 102111. [CrossRef]
29. Lv, Y.; Lou, S.; Tang, Z.; Liu, X.; Wang, X. Tunable C-band and L-band multi-wavelength erbium-doped fiber ring laser based on a triple-core photonic crystal fiber with polarization-dependent loss. *Opt. Laser Technol.* **2020**, *128*, 106269. [CrossRef]
30. Li, Y.; Shen, Y.; Tian, J.; Fu, Q.; Yao, Y. Wavelength Switchable Multi-Wavelength Erbium-Doped Fiber Laser Based on Polarization-Dependent Loss Modulation. *J. Light. Technol.* **2021**, *39*, 243–250. [CrossRef]
31. Huang, B.; Sheng, X.; Tang, Z.; Lou, S. High SMSR and widely tunable multi-wavelength erbium doped fiber laser based on cascaded filters. *Infrared Phys. Technol.* **2022**, *122*, 104082. [CrossRef]
32. Martinez-Ramirez, L.G.; Alvarado, E.S.; Gallegos-Arellano, E.; Fernandez-Jaramillo, A.; Estudillo-Ayala, J.; Jauregui-Vazquez, D.; Rojas-Laguna, R.; Sierra-Hernandez, J. Select-cutoff Mach-Zehnder interferometer based on waist-enlarged technique and its multi-wavelength fiber laser application. *Infrared Phys. Technol.* **2023**, *128*, 104508. [CrossRef]
33. Contreras-Teran, M.A.; Gallegos-Arellano, E.; Jauregui-Vazquez, D.; Martinez-Rios, A.; Hernandez-Garcia, J.C.; Ayona, J.R.R.; Sierra-Hernandez, J.M. Spacing mode multi-wavelength erbium doped fiber laser based on a symmetrical long-period fiber grating. *Phys. Scr.* **2024**, *99*, 095517. [CrossRef]

34. Zhang, W.; Liu, X.; Shi, Y.; Tong, Z.; Wang, X.; Wang, H. Spacing-adjustable and switchable multi-wavelength erbium-doped fiber laser using the filter of MMF–PMF–MMF based on PHB. *Appl. Phys. B Lasers Opt.* **2024**, *130*, 129. [CrossRef]
35. Qin, G.; Li, Q.; Wei, W.; Duan, J. Multi-wavelength tunable ring cavity fiber laser incorporated with a Mach–Zehnder interferometer filter based on waist-enlarged fiber bitapers. *Optik* **2021**, *248*, 168088. [CrossRef]
36. Salceda-Delgado, G.; Martinez-Rios, A.; Jimenez-Lizarraga, M.; Rodríguez-Carreón, V.; Selvas-Aguilar, R.; Sierra-Hernandez, J.; Rojas-Laguna, R.; López-Zenteno, J. Modifiable optical fiber tapered Mach–Zehnder interferometer for tune and switch optical fiber laser applications. *Opt. Fiber Technol.* **2022**, *70*, 102884. [CrossRef]
37. Al-Rubaiyee, H.A.; Al-Hayali, S.K.; Al-Janabi, A.H. Vernier effect based on hybrid fiber interferometers: A new tool for wavelength switchability and adjustable free spectral range fiber lasing. *Opt. Contin.* **2023**, *2*, 1203–1215. [CrossRef]
38. Al-Rubaiyee, H.A.; Al-Hayali, S.K.; Harun, S.W.; Al-Janabi, A.H. Vernier effect based on cascading two Mach–Zehnder interferometers for selectable comb filter and saturable absorber applications in erbium-doped fiber laser. *Opt. Fiber Technol.* **2024**, *84*, 103757. [CrossRef]
39. Gutierrez-Gutierrez, J.; Rojas-Laguna, R.; Estudillo-Ayala, J.; Sierra-Hernández, J.; Jauregui-Vazquez, D.; Vargas-Treviño, M.; Tepech-Carrillo, L.; Grajales-Coutiño, R. Switchable and multi-wavelength linear fiber laser based on Fabry-Perot and Mach-Zehnder interferometers. *Opt. Commun.* **2016**, *374*, 39–44. [CrossRef]
40. Zhao, Q.; Pei, L.; Zheng, J.; Tang, M.; Xie, Y.; Li, J.; Ning, T. Tunable and interval-adjustable multi-wavelength erbium-doped fiber laser based on cascaded filters with the assistance of NPR. *Opt. Laser Technol.* **2020**, *131*, 106387. [CrossRef]
41. Bianchetti, M.; Sierra-Hernandez, J.; Mata-Chavez, R.; Gallegos-Arellano, E.; Estudillo-Ayala, J.; Jauregui-Vazquez, D.; Fernandez-Jaramillo, A.; Salceda-Delgado, G.; Rojas-Laguna, R. Switchable multi-wavelength laser based on a core-offset Mach-Zehnder interferometer with non-zero dispersion-shifted fiber. *Opt. Laser Technol.* **2018**, *104*, 49–55. [CrossRef]
42. Martin-Vela, J.A.; Sierra-Hernandez, J.; Gallegos-Arellano, E.; Estudillo-Ayala, J.; Bianchetti, M.; Jauregui-Vazquez, D.; Reyes-Ayona, J.; Silva-Alvarado, E.; Rojas-Laguna, R. Switchable and tunable multi-wavelength fiber laser based on a core-offset aluminum coated Mach-Zehnder interferometer. *Opt. Laser Technol.* **2020**, *125*, 106039. [CrossRef]
43. Chang, Y.; Pei, L.; Ning, T.; Zheng, J.; Li, J.; Xie, C. Switchable and tunable multi-wavelength fiber ring laser employing a cascaded fiber filter. *Opt. Fiber Technol.* **2020**, *58*, 102240. [CrossRef]
44. Zhao, X.; Dong, M.; Zhang, Y.; Luo, F.; Zhu, L. Switchable multi-wavelength and tunable wavelength spacing erbium-doped fiber laser based on a phase-shifted fiber Bragg grating combined with a Mach-Zehnder interferometer. *Opt. Laser Technol.* **2019**, *112*, 500–507. [CrossRef]

Disclaimer/Publisher's Note: The statements, opinions and data contained in all publications are solely those of the individual author(s) and contributor(s) and not of MDPI and/or the editor(s). MDPI and/or the editor(s) disclaim responsibility for any injury to people or property resulting from any ideas, methods, instructions or products referred to in the content.